Open access • Journal Article • DOI:10.1049/IET-CDT.2015.0202

Mechanically-coupled ring-resonator filter and array (analytical and finite element model). — Source link

Vinayak Pachkawade, Rajesh C. Junghare, Rajendra M. Patrikar, Michael Kraft

Institutions: University of Liège

Published on: 01 Sep 2016 - Iet Computers and Digital Techniques (The Institution of Engineering and Technology)

Topics: Mechanical filter, Band-pass filter, Frequency response, Resonator and Bandwidth (signal processing)

Mechanically-Coupled Ring-Resonator Filter and Array (Analytical and Finite Element Model)

Vinayak Pachkawade [1*], Rajesh Junghare [2], Rajendra Patrikar [3] and Michael Kraft[4]

[1] [1] Montefiore Institute, Department of Electrical Engineering and Computer Science, University of Liege, 4000 Liege, Belgium
[2] Centre for VLSI and Nanotechnology, Visvesvaraya National Institute of Technology, Nagpur, India
[3] Professor: Centre for VLSI and Nanotechnology, Visvesvaraya National Institute of Technology, Nagpur, India
[4] Professor: Montefiore Institute, Department of Electrical Engineering and Computer Science, University of Liege, 4000 Liege, Belgium
[*] vinayak.pachkawade@gmail.com

Abstract: In this paper, a design of two MEMS based devices is carried out using an analytical and finite element analysis (FEA). The first device is mechanically-coupled ring-resonator bandpass filter with centre frequency of 4.4 MHz and a small bandwidth of only 36 kHz. Flexural-mode ring resonators have been mechanically coupled using soft mechanical spring for realizing the filtering action. Due to inherent symmetry in the ring structure, a relatively simple approach is used to access a low-velocity coupling locations as opposed to its clamped-clamped beam filter counterpart, where, a little mismatch in the position of coupling location near the anchors of clamped-clamped beam may result in a bandwidth change thereby affecting its performance. We also show a reduction in the amplitude of spurious mode by accentuating the filter structure in its fully-differential mode which is inherently present in the ring geometry. Moreover, the effect of the number of the support beams and structural damping on the frequency response of a filter has been analysed. A second device is mechanically-coupled ring-resonator arrays with varying number of rings coupled. The mechanical links (i.e., coupling elements) using short stubs connect each constituent resonator of an array to its adjacent ones at the high-velocity vibrating locations to accentuate the desired mode and reject all other spurious modes. Both analytical and finite element based simulation results for parameters of the designed structure are found in good agreement.

1. Introduction

Over the past few years, extensive efforts have been devoted to replace off-chip frequency-selective devices (i.e., frequency references and filters) in telecommunication systems with on-chip microelectromechanical systems (MEMS) based resonators. This is due to their high quality factors, linearity, compatibility with typical integrated circuit fabrication processes, etc. [1] [2] [3]. Various designs and fabrication platforms to realize micromechanical devices have been developed for analog signal processing in sensing and telecommunication applications [4] [5] [6]. Mechanical coupling techniques based on the coupling of individual mechanical resonators have been used for the implementation of higher order filters and have been applied to micromechanical resonators for filter synthesis. Researchers have modelled such structures by electrical equivalent circuit simulations to predict

the performance of the final device [7] [8]. Various filter structures operating at very high frequencies up to GHz range have been demonstrated [9]. Performance improving modelling techniques such as drumhead resonator based filter, contour-mode disk, stemless wine-glass-mode, differential disk-array has also been described to realize micromechanical bandpass filters with small bandwidth [10] [11] [12] [13]. Researchers have also demonstrated modelling and design of a filter with electrical coupling where instead of mechanical beam an electrical capacitor and/or an electrostatic capacitor transduction gap has been used to form a coupling between two mechanical vibrating resonators [14]. A filter coupling scheme, which combines the merits of mechanically and electrically coupled methods to enable a well-defined narrow bandwidth in a bandpass filter has also been demonstrated recently [15].

Based on the abovementioned state of the art of mechanical filter design, in the first part of this paper, a new type of mechanically-coupled flexural-mode ring-resonator based filter is presented. This bandpass filter is analytically designed and simulation results are found matching well with those of finite element based models. A filter is designed with a centre frequency of 4.4 MHz and a small bandwidth of 36 kHz. A soft mechanical spring has been used to couple two rings for realizing the bandpass filtering action. This structure also offers a differential mode of vibration. Due to inherent symmetry in the ring structure, a simple way to access low-velocity, i.e. low vibrational amplitude points, as coupling locations is proposed. This approach is relatively convenient as opposed to using clamped-clamped (CC) beam filters, where, a small mismatch during fabrication in the position of the coupling locations near the anchors of CC beam may result in a bandwidth change, thereby affecting its performance [16] [17].

Another important class of devices we designed is mechanically-coupled micromechanical resonator arrays that are popular for oscillator applications due to their lower motional resistance and higher power handling capabilities. Various resonator array configurations such as free-free beam array, corner- coupled square frame arrays, disk-arrays, etc. have been presented in the past and in recent times [18] [19] [20]. Therefore, in the second part of this work, mechanically-coupled flexural-mode ring-resonator arrays with varying number of rings coupled together are presented. The mechanical links (i.e., coupling elements) using short stubs connect each constituent resonator of an array to its adjacent ones at the high-velocity, i.e. high vibrational amplitude points as a coupling location to accentuate the desired mode and reject all other spurious modes.

We have demonstrated design, fabrication and measurement results of a flexural mode ring resonator with integrated electronics in previous work [21]. We have also shown in the same work that differential signalling scheme helps in a cancelling feedthrough associated with a capacitively-transduced resonators thereby improving signal-to-noise ratio, reducing motional resistance, impedance matching, etc.

In this paper, we present an analytical and a finite element analysis (FEA) of mechanically-coupled flexural mode ring resonator based filter and an array device. Our motivation is to model and design these devices and analyse their performance in order to utilize them as MEMS based building blocks for analog signal processing in sensing and telecommunication applications.

Beginning with a qualitative description of filters designed in this work in Section 2, the paper continues with the structural operation and design method of a 36 kHz bandwidth micromechanical ring bandpass filter. Section 3 explains structural operation and design method of an array of mutually coupled rings followed by conclusion and projections on future advancements of these mechanical devices in Section 4.

2. Mechanically-Coupled Ring-Resonator Filter

2.1. Bandpass Filter Structure And Operation

Fig. 1 presents a perspective view schematic of a two-ring resonator filter, along with appropriate bias, driving, and sensing ports. As shown, this filter consists of two identical flexural-mode ring resonators, coupled mechanically by a flexural-mode beam. Conducting electrodes for driving and sensing underlie the periphery regions of each resonator and serve as capacitive transducer electrodes positioned to induce out-of-plane resonator vibration. This, coupled two-resonator system exhibited two mechanical resonant modes with closely spaced frequencies that define the filter passband. The centre frequency of the filter was determined primarily by the frequencies of the constituent resonators, while the spacing between

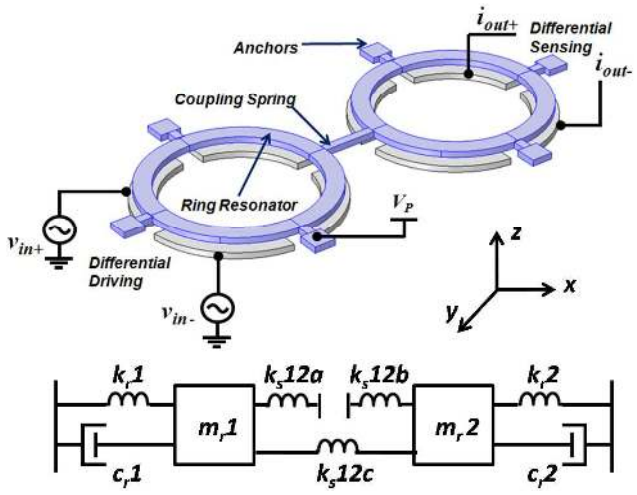

Fig. 1. (a) Perspective view schematic of a two flexural-mode ring resonator μmechanical filter, along with the preferred bias, excitation, and sensing circuitry. (b) The equivalent mechanical circuit.

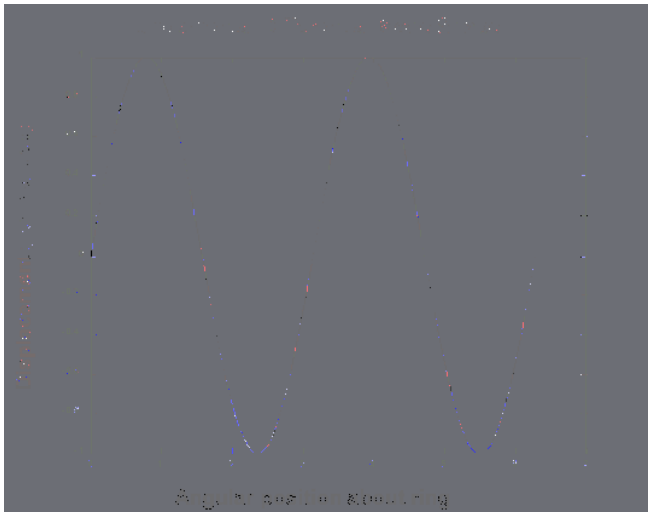

Fig. 2 Mode shape function analytically solved and plotted using MATLAB for flexural-mode ring-resonator.

modes (i.e., the bandwidth) was determined largely by the stiffness of the coupling spring. Quarter-wavelength ($\lambda/4$) coupling was used to alleviate mass loading effects caused by similar resonator and coupling dimensions [16].

In general, to operate this filter, differential ac input voltages v_{in}^{+} and v_{in}^{-} are applied to the two input electrodes as shown in Fig. 1(a). A DC bias V_p is then applied to the filter structure through anchors. The application of this input creates a z–directed electrostatic force between differential driving electrodes and the conductive resonator that induces z-directed vibration of the input resonator when the frequency of the input voltage comes within the passband of the mechanical filter. This vibrational energy is imparted to the output resonator via the coupling spring, causing it to vibrate as well. Vibration of the output resonator creates a dc-biased, time-varying capacitor between the conductive resonator and differential sensing output electrodes, which then sources output currents namely i_{out}^{+} and i_{out}^{-} sensed in differential way. Fig. 1(b) depicts an equivalent mechanical circuit for the filter structure. The following equations have been analytically solved to determine the resonance frequency and mode shape of a homogeneous, uniform, and an unsupported circular ring, respectively [13].

$$f_0 = \frac{i(i^2-1)}{2\pi R^2}\left\{\frac{EI_x}{m(i^2+\frac{EI_x}{GC}}\right\}^{\frac{1}{2}} \tag{1}$$

$$\begin{bmatrix} x \\ z \\ y \\ \theta \end{bmatrix} = \begin{bmatrix} 0 \\ \sin i\alpha \\ 0 \\ -\frac{i^2}{R}\left\{\frac{\frac{GC}{EI_x}}{1+i^2\frac{GC}{EI_x}}\right\}\sin i\alpha \end{bmatrix} \tag{2}$$

where i is the mode number; x, y, z, and θ are mode shapes corresponding to deformations parallel to x, y, z axes, and rotation about z axis, respectively; m is the mass per unit length of the ring; C is a torsion constant; E represents the modulus of elasticity; G is the shear modulus; I_x and I_y are area moments of inertia about x and y axes, respectively; R represents the radius to the mid-line of the ring; α is the angular position about the ring; μ is the mass density of the ring material; v is Poisson's ratio. For i = 2, the mechanical resonance frequency f_0 of a single resonator, which is also a centre frequency of the filter designed in this work was calculated. The calculated filter centre frequency, f_0 = 4.14 MHz was found to be matched with a finite element model (FEM) as will be shown later. Similarly, values for equivalent

mechanical elements, such as dynamic mass, spring, and damper, were also analytically determined using equations (3), (4), and (5), respectively.

$$m_{re}(z) = \frac{\rho W_r h \int_0^{2\pi} \left[Z_{\mathrm{mod}\,e}(\theta') \right]^2 d\theta'}{\left[Z_{\mathrm{mod}\,e}(\theta) \right]^2} \tag{3}$$

$$k_{re}(z) = \omega_0^{\,2} m_{re}(z) \tag{4}$$

$$c_{re}(z) = \frac{\sqrt{k_{re}(z) m_{re}(z)}}{Q} = \frac{\omega_0 m_{re}(z)}{Q} \tag{5}$$

Fig.2 shows a mode shape function (equation 2) of a flexural-mode ring resonator solved and plotted in MATLAB. From fig. 2, it can be seen that this structure offers a desired differential mode shape at resonant frequency that can be used to realize a differential mode ring-resonator based filter.

2.2. A 36 kHz Bandwidth Bandpass Filter Design

Fig. 3 shows a frequency spectrum for a 4.4 MHz mechanical flexural-mode ring-resonator filter plotted in MATLAB. A differential electrostatic force was applied to the two driving electrodes and in response vibration amplitude (displacement) was sensed by other two sensing electrodes. A differential mode was utilized since provides spurious mode reduction that may interfere in the passband of the filter response [21].

Fig. 4 shows a well-known spring softening effect for a 4.4 MHz mechanical flexural-mode ring-resonator filter. As shown, the resonance frequency of this device is tunable via adjustment of V_p, and this can be used advantageously to implement filters with tunable centre frequencies, or to correct for passband distortion caused by finite planar fabrication tolerances [16].

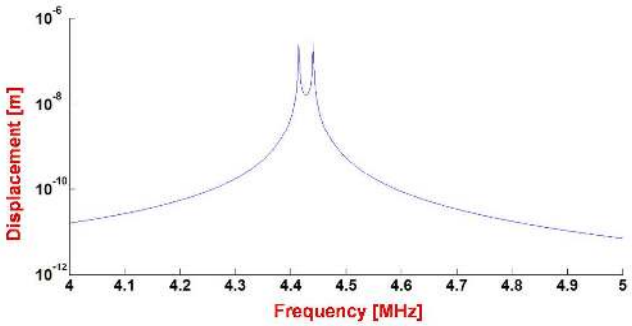

Fig. 3 Analytically determined frequency spectrum for a 4.4 MHz mechanical flexural-mode ring-resonator filter.

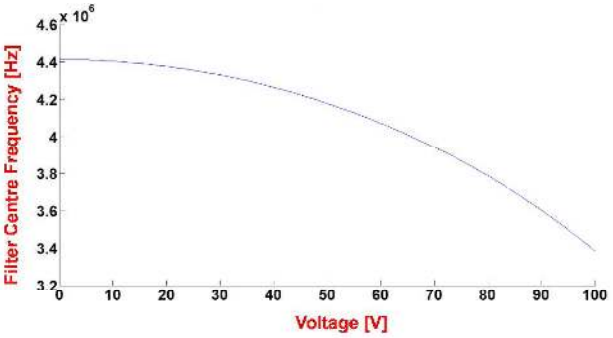

Fig. 4 Spring softening effect for a 4.4 MHz mechanical flexural-mode ring-resonator filter analytically modeled and plotted using MATLAB

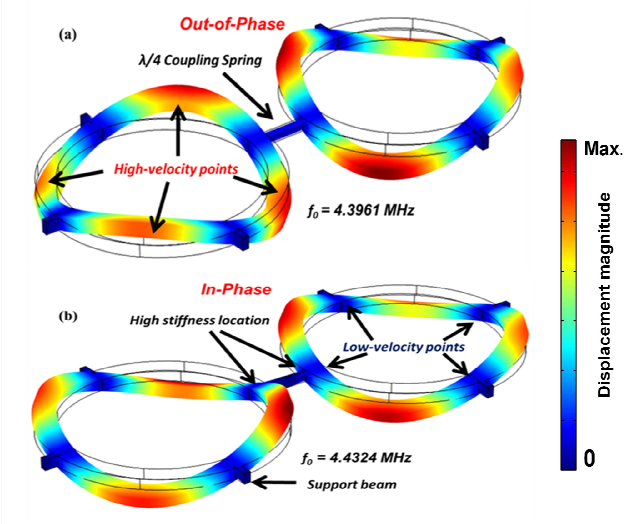

Fig. 5. 3-D plot of a vibrating mode shapes of a flexural-mode ring resonator mechanically coupled by $\lambda/4$ coupling spring. (a) Out-of-plane mode shape and (b) in-plane mode shape.

Fig. 5 shows a 3D plot of a vibrating mode shape of a flexural-mode ring resonator mechanically coupled with λ/4 coupling spring. This finite element model (FEM) was implemented using COMSOL. As shown in fig. 5, the structure vibrates at two closely spaced resonant frequencies. Resonators vibrate 180^0 out of phase at a frequency of 4.3961 MHz; whereas they vibrate in phase at a frequency of 4.4324 MHz. The centre frequency and bandwidth of this FEM was found matching with that of an analytical model implemented in MATLAB. Both high-velocity points (low-stiffness) and low-velocity points (high-stiffness) are indicated for the flexural-mode ring geometry.

The filter design is dominantly governed by the bandwidth equation [8] [16]

$$BW = \frac{ks_{12}}{k_{12}} \frac{f_0}{k_{rc}} \qquad (6)$$

where f_0 is the centre frequency of the filter, it is also the resonant frequency of each of the resonators, k_{12} is the normalized coupling coefficient (k_{ij} = 0.7225 [16]), ks_{12} is the coupling beam stiffness, and k_{rc} is the resonator effective stiffness at the coupling location. In our design, the effective stiffness is highest at the motionless nodal points of the resonator. From equation (6), it is obvious that the bandwidth depends only on the resonator stiffness, i.e., the coupling location on the resonators, and the coupling-beam stiffness. The other two parameters are constants. If the coupling is at a low-velocity location on the resonator, the effective mass increases and so is the effective stiffness; consequently, the filter bandwidth decreases [22]. In order to achieve a small bandwidth for the filter design, choosing the optimum coupling location plays an important role. It is realtively easy to determine the coupling location in this type of geometry due to the inherent symmetry of the ring structure where motionless nodal points (i.e. low-velocity points) are easy to locate. Moreover, the motionless nodal points do not change due to process variations as opposed to their clamped-clamped beam counterparts [16] [17].

2.3. Mode Coupling Spring Design Equation

Extensional and torsional-mode coupling spring elements have similar characteristic equations. The stiffness of the coupling beam is given by [22]

$$k_c = \omega A\sqrt{\rho E}$$
$$l = \frac{n\lambda}{4}, where \qquad (7)$$
$$n = 1,3,5.....$$

At the microscale, the mass of the coupling beam and that of the resonator are of the same order. As a result, it is important to account for the coupling-beam mass. As this is not an easy process, a simplier way is to set the spring length equal to an odd multiple of the quarter of the wavelength. By doing so, the coupling spring mass should have no effect on the resonant frequency [16] [22]. For the flexural-mode coupling with clamped ends, the beam stiffness is calculated using equation (8). Again, it is important to find the coupling-spring dimensions that correspond for the quarter-wavelength to eliminate the effect of the coupling-beam mass. As a result, the equality given by equation (9) should be satisfied.

$$k_c = \frac{EI\alpha^3(\sin\alpha + \sinh\alpha)}{L^3(\cos\alpha\cosh\alpha - 1)}, \qquad (8)$$
$$\alpha = \sqrt[4]{\frac{\rho A\omega^2}{EI}}L$$

$$H6 = \sin\alpha\cosh\alpha + \cos\alpha\sinh\alpha = 0 \qquad (9)$$

Based on the above analysis, a coupling spring corresponding to a "quarter-wavelength" of the filter centre frequency was designed.

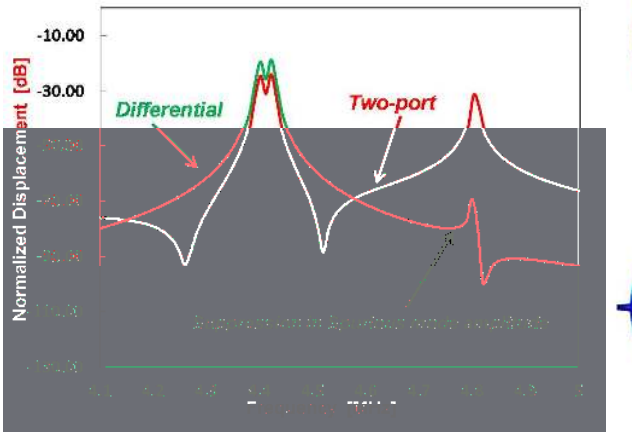

Fig.6 Simulated spectra (using Comsol Multiphysics) of ring microresonator filter under two different driving and sensing schemes.

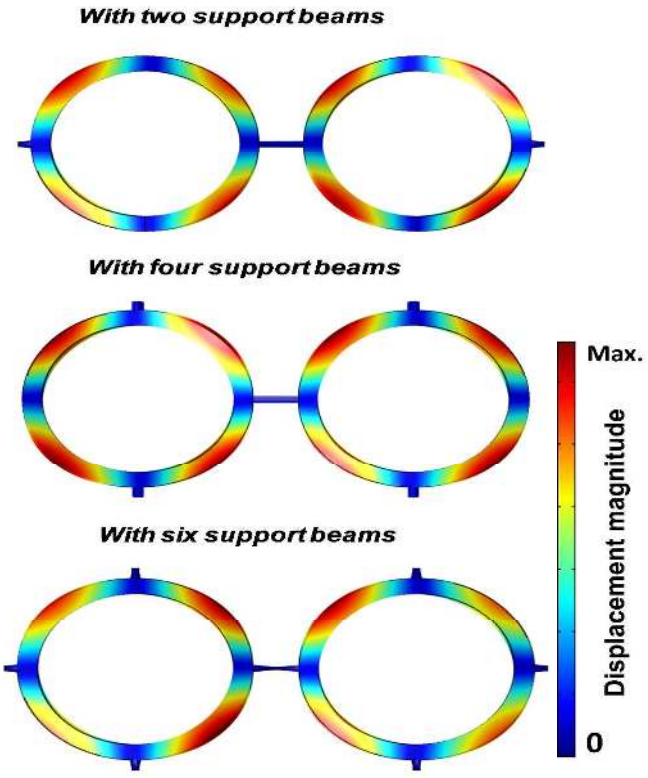

Fig.7 Vibrating mode shapes of a ring-resonator filter with no of support beams (a) with two support beams (b) with four support beams (c) with six support beams

Motionless nodal points of the ring were selected as the optimum coupling location(s) on the resonators to result in a narrow bandpass of a filter.

Fig. 6 presents a finite-element simulation of a proposed structure. As shown in Fig.6, using two ports a differential signaling scheme is applied for driving and sensing the signal to/from the filter. As stated above, the advantage of accentuating a structure in its fully differential mode helps reducing the vibration amplitude of spurious modes compared to its two-port driving and sensing scheme. A bandwidth of about 36 kHz was obtained which matches well with an analytical model discussed earlier. This is the smallest possible bandwidth that can be realized in this configuration of a filter. The centre frequency of the filter is seen to be 4.4 MHz.

2.4. Effect of Support Beams on Frequency Response and Quality factor of a Filter

Fig. 7 presents simulated vibrating mode shapes of a filter with 2, 4, and 6 support beams. As seen from fig. 7, it is possible to make a structure vibrate in differential mode shape even with only two support beams. This is expected to result in reduced anchor losses and therefore an increase in the quality factor. Fig. 8 represents the frequency response of a filter for varying number of support beams. The centre frequency of the filter is seen to decrease as fewer supports lead to reduced effective stiffness and therefore a decrease in the natural frequency of vibration. However, the bandwidth of a bandpass filter response in each case will also change in this case with respect to equations (6) and (8). Fig. 9 shows a wide-band (over a large frequency span) frequency response of a filter with varying number of support beams. We used the perfectly matched Layer (PML) method (discussed in next section 2.4.1) to estimate the support loss quality factor for desired and spurious modes in the ring resonator filter for varying

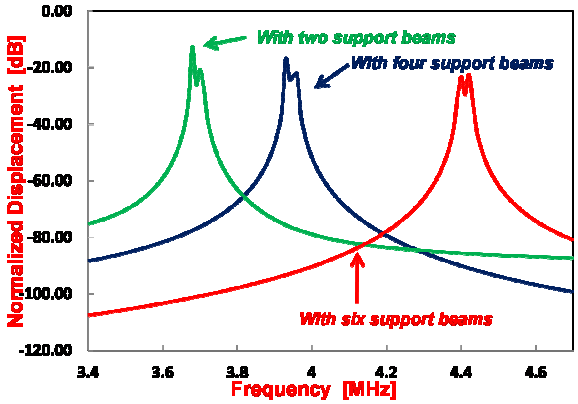

Fig.8 Simulated spectra (Comsol Multiphysics) of ring microresonator filter under three different number of support beam combinations.

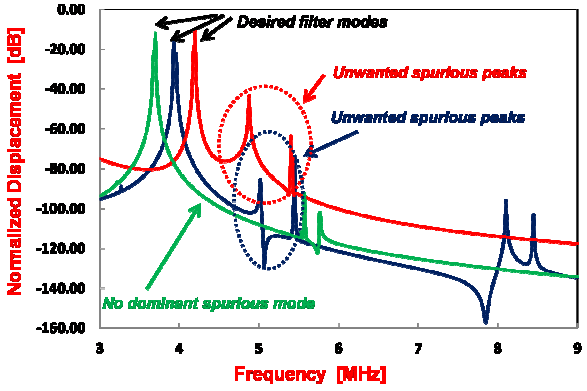

Fig.9 Simulated wide band spectra (using Comsol Multiphysics) of a ring microresonator filter with 2 (green), 4 (blue), and 6 (red) support beams. No dominant significant spurious mode was observed near the filter centre frequency particularly for the design using only 2 and 4 support beams. Quality factor for the desired mode was also seen to be higher than the spurious mode.

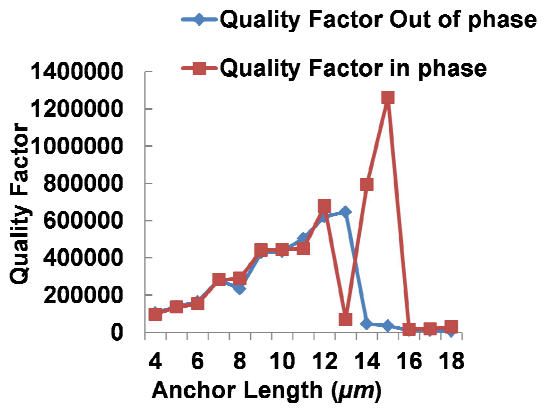

Fig.10. Simulated quality factor (Comsol Multiphysics) for length of substrate=200 and width of substrate=800

number of support beams.

The support loss quality factor in the ring resonators was found to be decreasing as its mode order increases. This is shown from the wide-band frequency spectrum in Fig. 9.

As said before, we designed support beams with geometries that isolate the resonator structure from its anchors in order to minimize energy losses to the substrate, allowing the structure to retain its optimum quality factor. This is effectively one possible way we could show a suppression/reduction in the amplitudes of the spurious modes. Secondly, in our design, a geometry-specific excitation configuration, i.e. (fully differential driving and sensing) has been purposefully deployed to suppress/remove the amplitudes of all undesired spurious modes around the centre frequencies of the stand-alone micromechanical flexural ring resonators.

Using these two techniques, we have attempted to show that spurious modes normally observed near the centre frequencies of stand-alone micromechanical flexural ring resonators could be suppressed or nearly completely removed. This is shown in Fig.9.

2.4.1 Anchor loss and Structural Damping effect

A designed mechanical resonator structure is supported by six torsional beams attached at its nodal points. Since they are attached at nodal points, the support springs (ideally) sustain no translational movement during resonator vibration and, thus, support (i.e., anchor) losses due to translational movements are considered negligible [17]. For this design, anchor losses have been modelled for a structure using two ring resonators coupled mechanically. At resonance, energy oscillates between these two resonators. This wave energy also passes through anchors to the substrate. This loss of energy is reduced with proper designing of anchors. The anchors in our design are placed at nodal points where displacement is ideally zero for the ring.

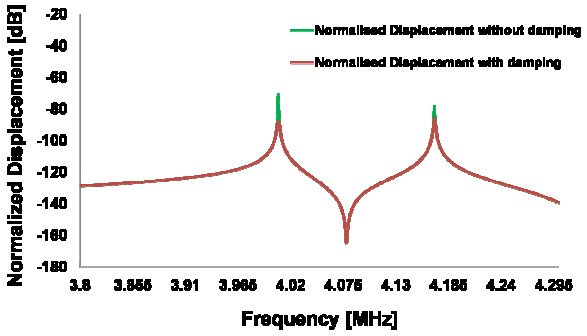

Fig.11 Simulated spectra (using Comsol Multiphysics) of ring microresonator filter with and without damping.

We used the method of PML (Perfectly matched Layer) in COMSOL to calculate the *Q*-

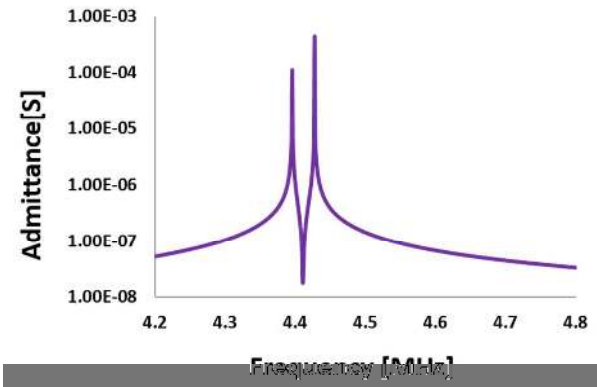

Fig.12 An admittance plot (Comsol Multiphysics) of ring microresonator filter under an applied voltage.

factor as a result of support-losses [23].In our FEM analysis of a structure, PML is enclosing the substrate. The PML absorbs all waves and does not reflect the waves. In FEM simulation, substrate was made much larger in size as compared to resonator structure so that modelling results come closer to reality. Fig. 10 shows the quality factor verses changing anchor length. In analysis, it was found that anchor length greater than 13μm does not give good quality factor. To achieve highest quality factor for both in phase and out of phase mode, anchor length between 11um to 12um should be chosen as shown in Fig.10.

Finally, Fig.11. shows a FEM simulated spectra of ring microresonator filter with and without damping. In FEM analysis, Rayleigh damping model and material constants were defined to model the material losses for this structure. In the Rayleigh damping model, the damping coefficient c is related to the mass, m, and the stiffness, k, by the equation:

$$c = \alpha_{dM} m + \beta_{dK} k \text{ ---------- (10)}$$

where, $\alpha_{dM} m$ and $\beta_{dK} k$ are two material constants required to model damping effect [24].

2.5. Electromechanical model of a ring-resonator Filter

An interface between the mechanical and electrostatical building blocks was created in the electromechanics module of COMSOL. This model showed the response of a filter under an applied electrostatic load and computed the deformation of the ring due to the applied voltage. A bias voltage Vp = 45V was applied to the ring structure via an anchor, as can be seen from the perspective view schematic of a two flexural-mode ring resonator mechanical filter, along with the bias, excitation, and sensing circuitry. (Fig.1 (a)). A system ground was created and an admittance plot was obtained as shown in Fig.12. The device geometry and the materials used for this resonator filter are listed in Table 1.

To flatten the filter passband in Fig.12, the quality factors of the end resonators should be loaded via resistive termination with a value of R_Q given by [16]:

$$R_Q = \left(\frac{Q_r}{qQ_f} - 1\right).R_x \approx \frac{Q_r}{qQ_f}.\frac{m_r\omega_o}{Q\eta_e^2} \approx \frac{m_r BW}{q\eta_e^2} \qquad (11)$$

where, R_x is the motional resistance of a constituent end ring resonator; Q is the unloaded quality factor of the resonator; $Q_{filter} = f_o/BW$, BW the filter bandwidth; q the normalized parameter obtained from the reference [16]; m_r the dynamic mass of the ring resonator at its point of maximum displacement; and η_e the electromechanical coupling factor. For our design, the analytically determined value of the termination resistor is $R_Q \approx 240$ kΩ.

To attain low-loss capacitive resonators implemented as a filter, the considerable R_x for such a capacitive device can be significantly reduced by choosing appropriate values for the Q-factor, the electromechanical transduction factor, η_e, and the capacitive gap, (analytically determined values are listed in Table 1) thus relaxing the requirement of the termination resistance (R_Q) for the impedance matching of a given filter.

3. Mechanically-Coupled Ring-Resonator Array

Fig. 13 presents the vibrating mode shape of the resonator array obtained via finite element simulation. Mechanically coupled locations are shown, indicating the high-velocity (i.e. large-vibration-amplitude) coupling approach. The major advantages of this resonator array design mainly come from 1) differential transduction to effectively reduce the feedthrough while improving signal-to-noise-ratio as shown in our previous work [21] and 2) higher power handling capability compared with that of a single resonator because the maximum handling power is proportional to the effective stiffness, *k*eff, of the device, where *k*eff of an N-resonator array is N times larger than that of a single resonator [18]. Furthermore, designing a mechanically coupled resonator array is a superior way to lower the motional resistance by summing the output motional current of every identical resonator in an array [18] [19] [20].

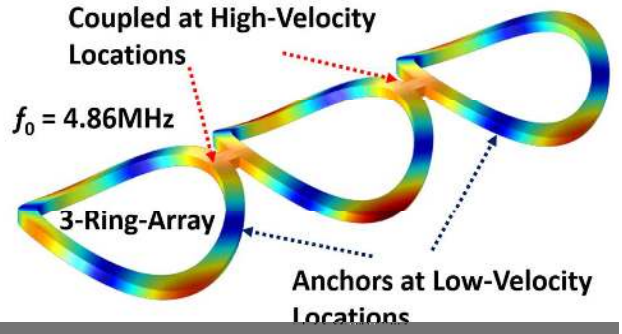

Fig.13 (a) Vibrating mode shape of a resonator array with 3 resonators mechanically coupled together.

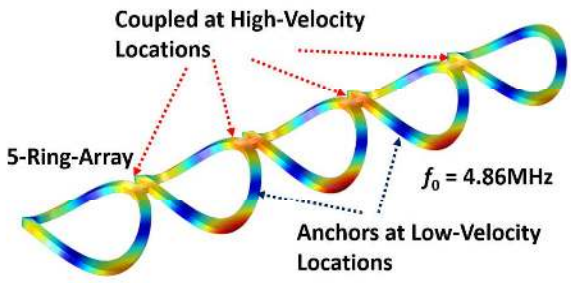

Fig. 13 (b) Vibrating mode shape of a resonator array with 5 resonators mechanically coupled together.

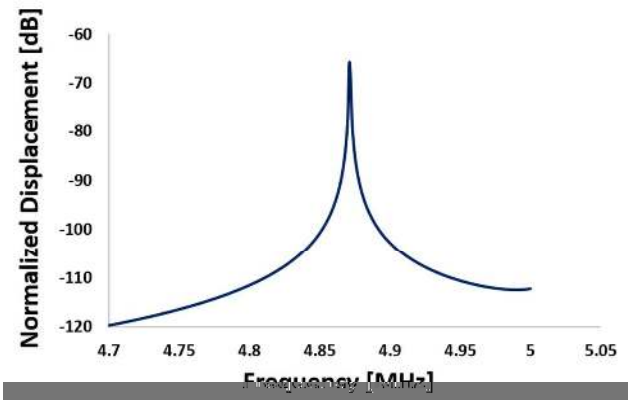

Fig. 14. The simulated frequency spectra of multiresonator arrays under the applied force of 1×10^{-9} N.

To create the mechanically coupled resonator array, identical resonators are placed near each other, and each constituent resonator is connected to its adjacent ones by mechanical coupling links, as shown in Figs. 13(a) and 13(b). It implements additional high-velocity couplers (i.e., strong coupling) into the array because the coupling locations are at maximum velocity (or displacement) positions under ring vibration. It should be noted that high-velocity locations are the same as the large-vibration-amplitude locations where mechanical couplers create strong coupling among the constituent resonators of an array because of their maximized vibratory momentum [18].

The resonance frequency of a resonator array is very similar to that of a single resonator if all of the constituent resonators of the array operate in phase. In our design, it is 4.86 MHz as shown in Fig. 13(a) and 13(b). Anchors (not shown) can be placed at low velocity (or displacement) positions. Since anchors are not shown to be added to the structure, fixed mechanical boundary conditions were chosen by selecting edges of the rings in the solid mechanics module. To eliminate the spurious modes, stiff mechanical coupling elements (half wavelength couplers or short stubs at high-velocity vibrating locations) can be used to effectively push the spurious modes far away from the desired frequency [18]; in addition, differential electrical phasing design (inherent in this ring structure) also helps to select only one vibrating mode and reject all of the others [21]. Frequency domain analysis of this array structure was performed to determine eigen-frequencies and the resonator transfer function. To operate this array, a vibrating mode shape, as shown in Fig. 13, was chosen for differential driving and sensing. A differential force is applied to the two driving electrodes and in response vibration amplitude (displacement) is sensed by other two sensing electrodes. Unlike a filter structure shown in the first part of this paper, all the constituent resonators in an array are driven and sensed at the same time. Fig. 14 presents the simulated frequency spectra of multiresonator arrays under the device boundary load (applied force of 1×10^{-9} N). Device geometry and the materials used for this resonator array also are listed in Table 1.

Finally, Table 1 presents a performance summary of the analytical and FEM based models of a 1) mechanically-coupled, small bandwidth of only 36 kHz ring-based bandpass filter and 2) mechanically-coupled ring-resonator array. All device dimensions for a filter and array are mentioned. A surface

micromachining fabrication process [16] with polysilicon as a structural material can be utilized to realize the MEMS components. Also, a standard CMOS-MEMS fabrication process that has an advantage of integration with electronics on a single-chip can also be used to develop a prototype of these designs [17] [21].

Table 1 RING RESONATOR MICROMECHANICAL ARRAY AND FILTER SUMMARY

Parameter	Value		Units	Parameter	Value		Units
	Design/ Calculated	Simulated			Design/ Calculated	Simulated	
Outer radius, R_o (μm)	36	36	μm	Applied force in filter	1×10^{-6}	1×10^{-6}	N
Inner radius, R_i (μm)	30	30	μm	Normalized displacement	(-20)	-20	dB
Thickness, h (μm)	3.94	3.94	μm	Applied Voltage	45	45	V
Short stub length	4	4	μm	Filter termination resistor, R_Q	(240)	-	$k\Omega$
Short stub width	2	2	μm	Array centre frequency, f_{array}	(4.81)	4.86	MHz
Coupling spring length	(1.4)	1.4	μm	Applied force in array	1×10^{-9}	1×10^{-9}	N
Coupling spring width	(1)	1	μm	Normalized displacement	(-70)	-70	dB
Coupling spring stiffness, k_c	(61.34)	61.34	N/m	Resonator dynamic mass, m_{re}	(1.353×10^{-11})	-	kg
Young's modulus, E	160	160	GPa	Resonator dynamic stiffness, k_{re}	(1.04×10^{-4})	-	N/m
Density of Polysilicon, ρ	2330	2330	kg/m^3	Resonator dynamic damper, c_{re}	(6.25×10^{-8})	-	-
Poisson's ratio, rho	0.22	0.22	-	Filter Percent bandwidth, P_{BW}	(0.81)	-	%
Capacitive gap spacing	0.295	0.295	μm	Support beam length	(1.39)	1.39	μm
Bandwidth, BW	(36)	36	kHz	Support beam width	1	1	μm
Filter centre frequency , f_c	(4.541)	4.414	MHz	Electromechanical transduction factor, η_e	(1.42×10^{-6})	-	-
Normalized coupling coefficient, k_{ij}	0.7225	-	-	() **Indicates analytically calculated values**			

4. Conclusion

An inherent differential vibrational mode present in the flexural-type ring-resonator was utilized for designing two MEMS based components i.e. a filter and an array. In the first part of this paper, a small bandwidth micromechanical ring-resonator based bandpass filter that can be easily prototyped using a standard MEMS foundry process is presented. A small bandwidth of 36 kHz has been shown to be achievable by taking the advantage of symmetry in the ring geometry, which has a differential mode of vibration. By mechanically coupling two such rings at its lowest velocity points via quarter-wavelength coupling springs a bandpass filter is designed. This approach is more suited as compared to a filter realized using standard clamped-clamped beam resonators. In clamped-clamped beam based filter design, one has to precisely calculate a position over a length of a beam to mechanically couple the resonators. During fabrication, a small mismatch in the position, where, resonator beams are coupled may result in change in

the filter centre frequency and also a bandwidth. In the second part of the paper, micromechanical resonator arrays with varying number of rings coupled are presented. The mechanical links (i.e., coupling elements) using short stubs connect each constituent resonator of an array to its adjacent ones at the high-velocity vibrating locations to accentuate the desired mode at 4.86 MHz and reject all other spurious modes. Future projection on this work would be to elaborate on the analytical solution of a system and to fabricate this structure and compare the model with measurement results. We also plan to couple several such rings together at their high-velocity locations to form a 1-D array and then couple several 1-D arrays together at their low-velocity locations to design a 2-D array based filter that would benefit motional resistance and overall power handling capability of such a MEMS device.

5. References

[1] C.T.C.Nguyen, “Vibrating RF MEMS overview: Applications to Wireless Communications,” Proceedings, Photonics West:MOEMS-MEMS 2005, San Jose, California, January 22-27, 2005, Paper No. 5715-201.

[2] C.T.C.Nguyen, “Micromechanical Filters for Miniaturized Low-Power Communications,” Proceedings of SPIE: Smart Structures and Materials (Smart Electronics and MEMS), Newport Beach, California, March 1-5, 1999.

[3] E.R.Crespin, “Fully Integrated Switchable Filter Banks,” IEEE International. Microwave. Symposium, June 2012, pp.1-3.

[4] A.C.Wong, J.R.Clark, and C.T.C.Nguyen, “Anneal-activated, Tunable, 65 MHz Micromechanical Filters” Digest of Technical Papers, 10th International Conference on Solid-State Sensors and Actuators, Sendai, Japan, June 7-10, 1999, pp.1390-1393.

[5] B.Kim, R.H.Olsson III, and K.E.Wojciechowski, “AlN Microresonator-Based Filters with Multiple Bandwidths at Low Inter-midate Frequencies,”Journal of Microelectromechanical Systems, Vol. 22, no. 4, August 2013, pp.949-961.

[6] S.Gong and G.Piazza, “Design and Analysis of Lithium-Niobate-based High Electromechanical Coupling RF-MEMS Resonators for Wide-band Filtering,” IEEE Transaction on.Microwave.Theory Techology, Vol. 61, no.1, January 2013, pp.403-414.

[7] J.Burgess, "Mechanical Filters in Electronics", IEEE Transactions on Acoustics, Speech and signal Processing, Vol.32, no.1, February 1984, pp.191-191.

[8] K.Wang and C.T.C.Nguyen,"High-order Medium Frequency Micromechanical Electronic Filters," Journal of Microelectromechanical Systems, Vol.8, no.4, December 1999,pp.534-556.

[9] J.Wang, Z.Ren and C.T.C.Nguyen, "Self-aligned 1.14-GHz Vibrating Radial-mode Disk Resonators," Digest of Technical Papers, The 12th International Conference on Solid-State Sensors & Actuators (Transducers’03), Boston, Massachusetts, June 8-12, 2003, pp.947-950.

[10] D.S.Greywall and P.A.Busch, “Coupled Micromechanical Drumhead Resonators with Practical Applications as Electromechanical Bandpass Filters”, Journal of Micromechanics and Microengineering, Vol.12, no.6, October 2002, pp.925-938.

[11] J.R.Clark, W.T.Hsu, and C.T.C.Nguyen, "High-Q VHF Micromechanical Contour-mode Disk Resonators," in Electron Devices Meeting, Technical Digest International, December 10-13, 2000, pp.493-496.

[12] M.A.Abdelmoneum, M.U.Demirci, and C.T.C.Nguyen, "Stemless Wine-glass-mode Disk Micromechanical Resonators," The 16th Annual International Conference on MicroElectro Mechanical Systems, MEMS-03 Kyoto, IEEE, 19-23 January. 2003,pp.698-701.

[13] S.S.Li, Y.W.Lin, Z.Ren, and C.T.C.Nguyen, "An MSI Micromechanical Differential Disk-array Filter," Digest of Technical Papers, The 14th International Conference on Solid-State Sensors & Actuators (Transducers'07), Lyon, France, June 10-14, 2007, pp.307-311.

[14] S.Pourkamali, R.Abdolvand, and F.Ayazi, "A 600 kHz Electrically Coupled MEMS Bandpass Filter," in Proceedings, IEEE 16th International Conference on MicroElectroMechanical Systems (MEMS), Kyoto, Japan, January 2003, pp.702-705.

[15] C.Y.Chen, M.H.Li, C.H.Chin, C.S.Li, and S.S.Li, "Combined Electrical and Mechanical Coupling for Mode-Reconfigurable CMOS-MEMS Filters," in Proceedings, IEEE 27th International Conference on MicroElectroMechanical Systems (MEMS), San Francisco, CA, USA, January 2014, pp.1249-1252.

[16] F.D.Bannon III, J.R.Clark, and C.T.C.Nguyen, "High-Q HF Microelectromechanical Filters," IEEE Journal of Solid-Stare Circuits, Vol.35, no.4, April 2000, pp.512-526.

[17] J.L.Lopez, J.Verd, A.Uranga, J.Giner, G.Murillo, and F.Torres, "A CMOS-MEMS RF-tunable Bandpass Filter Based on two High-*Q* 22-MHz Polysilicon Clamped-clamped Beam Resonators," IEEE Electron Device Letters, Vol.30, no.7, July 2009, pp.718-720.

[18] M.H.Li, W.C.Chen,and S.S.Li, "Mechanically Coupled CMOS-MEMS Free-free Beam Resonator Arrays with Enhanced Power Handling Capability", IEEE Transactions on Ultrasonics, Ferroelectrics, and Frequency Control, 2012, Vol 59, Issue:3, pp.346-357.

[19] M.Demirci and C.T.C.Nguyen, "Mechanically Corner-coupled Square Microresonator Array for Reduced Series Motional Resistance,"IEEE/ASME Journal of Microelectromechanical System, Vol.15, no.6, December 2006, pp.1419-1436.

[20] S.Lee and C.T.C.Nguyen, "Mechanically-coupled Micromechanical Arrays for Improved Phase Noise," Proceedings, Joint Conference on IEEE International Ultrasonics, Ferroelectrics, and Frequency Control, 50th Anniversary, Montreal, Canada, August 2004, pp.280-286.

[21] V.Pachkawade, C.S.Li and S.S.Li, "A Fully-Differential CMOS-MEMS Resonator Integrated with an On-chip Amplifier," IEEE Sensors, Taipei, Taiwan, October 28-31, 2012, pp.1-4.

[22] M.Shalaby, M.Abdelmoneum and K.Saitou, "Design of Spring Coupling for High Q, High Frequency MEMS Filters," ASME 2006 International Mechanical Engineering Congress and Exposition Microelectromechanical Systems Chicago, Illinois, USA, November 5-10, 2006.

[23] D.S.Bindel and S.Govindjee, "Elastic PMLs for Resonator Anchor Loss Simulation," International Journal of Numerical Methods in Engineering, 2005, pp.789-818.

[24] Retrieved from http://www.comsol.com/